ISSN 1070-3284, Russian Journal of Coordination Chemistry, 2020, Vol. 46, No. 12, pp. 828–837. © Pleiades Publishing, Ltd., 2020.
Russian Text © The Author(s), 2020, published in Koordinatsionnaya Khimiya, 2020, Vol. 46, No. 12, pp. 749–757.

Binding of Gold(III) from Solutions by Tetranuclear Lead(II) Dipropyldithiocarbamate $[Pb_4\{S_2CN(C_3H_7)_2\}_8]$ and Chemisorption Synthesis of the Double Ionic Polymer Complex $([Au\{S_2CN(C_3H_7)_2\}_2][PbCl_3] \cdot 0.5CH_3{-}C_6H_5)_n$: Heteronuclear ($^{13}C$, ^{15}N) CP-MAS NMR, Structural Organization, and Construction Principles of Cationic and Anionic Polymer Chains

A. V. Ivanov[a], *, A. S. Zaeva[a], and A. I. Smolentsev[b, c]

[a] *Institute of Geology and Nature Management, Far East Branch, Russian Academy of Sciences, Blagoveschensk, 675000 Russia*
[b] *Nikolaev Institute of Inorganic Chemistry, Siberian Branch, Russian Academy of Sciences, Novosibirsk, 630090 Russia*
[c] *Novosibirsk State University, Novosibirsk, 630090 Russia*
**e-mail: alexander.v.ivanov@chemist.com*

Received January 24, 2020; revised February 28, 2020; accepted March 11, 2020

Abstract—Solid-state ^{13}C and ^{15}N CP-MAS NMR data adequately reflected the presence of four nonequivalent PrDtc ligands in the tetranuclear lead(II) *N*,*N*-dipropyldithiocarbamate (PrDtc), $[Pb_4\{S_2CN(C_3H_7)_2\}_8]$ (**I**); the spin–spin coupling constants $^3J(^{15}N{-}^{207}Pb)$ for the ligands were estimated. It was shown by ^{13}C MAS NMR that the chemisorption binding of $AuCl_3$ from a solution in 2M HCl using lead(II) dipropyldithiocarbamate is accompanied by complete redistribution of the PrDtc ligands from Pb(II) to Au(III) coordination sphere; this gives the double complex of $[Au\{S_2CN(C_3H_7)_2\}_2][PbCl_3]$ (**II**). Upon crystallization from an acetone–toluene mixture (3 : 1), this complex was isolated as the solvated form $([Au\{S_2CN(C_3H_7)_2\}_2][PbCl_3] \cdot 1/2CH_3C_6H_5)_n$ (**IIa**), which was characterized by X-ray diffraction (CIF file CCDC no. 1978947). The cationic part of the complex is represented by non-centrosymmetric gold(III) complex ions, $[Au\{S_2CN(C_3H_7)_2\}_2]^+$, which are combined by pairs of nonequivalent Au···S secondary bonds, thus forming supramolecular pseudo-polymer chain $([Au\{S_2CN(C_3H_7)_2\}_2]^+)_n$. The 1D polymeric trichloroplumbate(II) anion, $\{[Pb(\mu_2\text{-}Cl)_3]^-\}_n$, acts as the counter-ion. The C–H···Cl hydrogen bonds between the anionic and cationic chains lead to formation of channels in the crystal lattice, which are occupied by solvating toluene molecules.

Keywords: lead(II) dialkyldithiocarbamates, chemisorption synthesis, gold(III)–lead(II) double complexes, supramolecular self-organization, Au···S secondary bonds

DOI: 10.1134/S1070328420110032

INTRODUCTION

Despite their toxicity, lead and its compounds are widely used in the manufacture of electric batteries; they can also be used for fabricating highly efficient solar cells [1] and as additives enhancing protection against γ-radiation for some types of concrete [2]. In addition, Pb^{2+} ions were found to be beneficial for increasing the productivity of the bacteria *Paenibacillus polymyxa* in the biosynthesis of antibiotics [3]. From the practical standpoint, lead(II) dithiocarbamates are of interest as precursors for the one-step thermochemical syntheses of film and nano-scale lead sulfides [4–7] (crystalline PbS exhibits semiconducting properties and, therefore, it can be used to design optoelectronic devices). Lead(II) dialkyl(alkylene)dithiocarbamates that have been structurally characterized to date are not numerous: $[Pb(S_2CNR_2)_2]$ (R = CH_3 [8], C_2H_5 [9], C_3H_7 [10], *iso*-C_3H_7 [11, 12], C_5H_{11} [13], *cyclo*-C_6H_{11} [14]; R_2 = C_2H_5, *iso*-C_3H_7 [15], CH_3, $CH_2{-}C_6H_5$ [14, 16], C_2H_5, C_6H_5 [16], and $(CH_2)_4$ [17]).[1]

Previously, we found that dithiocarbamates of post-transition metal (Tl^+, Bi^{3+}) are able to efficiently capture gold(III) from solutions, which results in the formation of the corresponding Au(III)–Bi(III) [19, 20] and Au(III)–Tl(III) [21, 22] double complexes. As a continuation of this research, here we studied the reaction between freshly precipitated tetranuclear

[1] The structure of $[Pb\{Se_2CN(C_2H_5)_2\}_2]$ incorporating diselenocarbamate ligands is also known [18].

lead(II) dipropyldithiocarbamate, $[Pb_4\{S_2CN(C_3H_7)_2\}_8]$ (**I**), and an $AuCl_3$/2 M HCl solution. The reaction afforded the double complex of $[Au\{S_2CN(C_3H_7)_2\}_2][PbCl_3]$ (**II**) as an individual fixation mode of gold(III) from solutions. The solvated form of this complex, $[Au\{S_2CN(C_3H_7)_2\}_2][PbCl_3] \cdot 0.5CH_3C_6H_5$ (**IIa**), exhibits an ionic structure comprising alternation of anionic polymeric chains $([PbCl_3]^-)_n$ and cationic pseudo-polymeric chains $([Au\{S_2CN(C_3H_7)_2\}_2]^+)_n$. Compounds **I** and **II** were characterized by heteronuclear (^{13}C, ^{15}N) CP-MAS NMR spectroscopy.

EXPERIMENTAL

Initial sodium *N*,*N*-dipropyldithiocarbamate $Na\{S_2CN(C_3H_7)_2\} \cdot H_2O$ was prepared by reactions of equimolar amounts of $(C_3H_7)_2NH$ (Merck) and carbon disulfide (Merck) in an alkaline medium [23].

CP-MAS ^{13}C NMR (δ, ppm) for $Na\{S_2CN(C_3H_7)_2\} \cdot H_2O$: 208.3 ($-S_2CN=$); 59.4, 57.9 (1 : 1, $=NCH_2-$); 22.3, 21.5 (1 : 1, $-CH_2-$); 12.6, 11.5 (1 : 1, $-CH_3$) [24].

Synthesis of I, II, and IIa. Tetranuclear lead(II) complex **I** was prepared by precipitation of Pb^{2+} cations from the aqueous phase by sodium dipropyldithiocarbamate [10] and identified by ^{13}C and ^{15}N CP-MAS NMR (δ, ppm): 204.6, 202.5 (1 : 3, $-S_2\mathbf{C}N=$); 56.5, 55.4, 51.1 (1 : 1 : 2, $=N\mathbf{C}H_2-$); 22.6, 21.4, 21.1 (1 : 1 : 2, $-\mathbf{C}H_2-$); 13.8, 13.5, 13.1, 12.8, 12.3, 12.0, 11.6 ($-\mathbf{C}H_3$); 144.1 (17)*, 141.4 (16)*, 139.6 (24)*, 138.3 (15)* (1 : 1 : 1 : 1, $-S_2C\mathbf{N}=$), where * denotes spin–spin coupling constant $^3J(^{15}N-^{207}Pb)$, Hz.

The double Au(III)–Pb(II) complex **II** was prepared by chemisorption of gold(III) from a solution into a solid phase by freshly precipitated lead(II) dipropyldithiocarbamate according to the reaction

$$[Pb_4\{S_2CN(C_3H_7)_2\}_8] + 4H[AuCl_4] = 4[Au\{S_2CN(C_3H_7)_2\}_2][PbCl_3] + 4HCl.$$

A solution of $AuCl_3$/2 M HCl (5 mL) containing gold (35.46 mg) was added to freshly precipitated $[Pb_4\{S_2CN(C_3H_7)_2\}_8]$ (100 mg), and the mixture was magnetically stirred for 1 h. The resulting grayish-yellow finely crystalline precipitate was collected on a filter, washed with water, and dried on a filter. The residual gold content in the solution was determined using an iCE 3000 atomic absorption spectrometer (Thermo Electron Corporation, USA). The degree of gold binding from the solution was 93.6%. Although gold(III) sorbed from the solution to the solid phase (33.20 mg) determined the yield of **II** in 94.4% (with the expected weight of the complex of 145.54 mg), the experimentally obtained yield was only 127.35 mg (82.6%).

According to ^{13}C CP-MAS NMR data for **II** (δ, ppm): 197.4, 195.0 (1 : 1, $-S_2CN=$); 55.4, 53.7 ($=NCH_2-$); 22.0 ($-CH_2-$); 13.1, 11.8, 10.7 ($-CH_3$).

IR spectrum of **II** (KBr; ν, cm^{-1}): 2967 s, 2930 m, 2871 m, 1551 vs, 1464 m, 1449 m, 1439 m, 1361 m, 1308 m, 1274 w, 1252 s, 1194 m, 1161 m, 1103 m, 1086 m, 968 w, 895 m, 751 m, 608 m.

The single crystals for the X-ray diffraction experiment were prepared by dissolving the dried finely crystalline precipitate of the Au(III)–Pb(II) complex in an acetone–toluene mixture (3 : 1). The transparent yellow needle crystals of bis(*N*,*N*-dipropyldithiocarbamato-*S*,*S*')gold(III) *catena*-poly[tri(μ_2-chloro)-plumbate(II)] were formed in the solvated form **IIa** as a result of slow evaporation of the solvents at room temperature.

The $^{13}C/^{15}N$ CP-MAS NMR spectra were recorded on an CMX-360 spectrometer (Agilent/Varian/Chemagnetics InfinityPlus) operating at 90.52/36.48 MHz using a superconducting magnet (B_0 = 8.46 T) and Fourier transformation. Cross-polarization (CP) from protons was used: $^1H-^{13}C/^1H-^{15}N$ contact time of 2.00/1.25 ms. Proton decoupling for the suppression of $^{13}C-^1H/^{15}N-^1H$ interactions using the radio-frequency field at the proton resonance frequency (400.21 MHz) was applied [25]. Polycrystalline samples **I** and **II** weighing ~60/25 mg was placed into a 4.0 mm ZrO_2 ceramic rotor. The $^{13}C/^{15}N$ NMR measurements were performed using magic angle spinning (MAS) at a frequency of 5000–10100/3750(1) Hz; the proton π/2 pulse durations were 4.5–5.0/5.0 μs; 6100–10000/12100 transients, spaced by relaxation delays of 2.0/3.0 s, were accumulated. The isotropic chemical shifts $\delta(^{13}C)/\delta(^{15}N)$ were referred to one of components of the external standard, crystalline adamantane (δ = 38.48 ppm relative to tetramethylsilane)/crystalline NH_4Cl (δ = 0.0 ppm; –341 ppm on the absolute scale [26]) with the correction for magnetic field drift using a frequency equivalent of 0.051/0.018 Hz/h. The magnetic field homogeneity was verified by monitoring the adamantane reference line width (2.6 Hz).

FT-IR spectra were measured on an interferential FSM-1201 spectrometer in the 400–4000 cm^{-1} range (KBr pellets). The instrument control and processing of the spectra were performed using the FSpec program (version 4.0.0.2 for Windows, LLC Monitoring, Russia).

X-ray diffraction study of complex **IIa** was carried out for yellow needle single crystals on a Bruker-Nonius X8 Apex CCD diffractometer (MoK_α radiation, λ = 0.71073 Å, graphite monochromator) at 150(2) K. The data were collected by the standard procedure: φ- and ω-scanning of narrow frames. The absorption corrections were applied empirically using the SADABS software program [27]. The structure was solved by direct methods and refined by the least

Table 1. Crystallographic data and X-ray experiment and structure refinement details for **IIa**

Parameter	Value
Molecular Formula	$C_{17.5}H_{32}N_2S_4Cl_3PbAu$
M	909.20
System	Orthorhombic
Space group	*Pbcn*
a, Å	7.7670(7)
b, Å	25.885(2)
c, Å	28.276(2)
β, deg	90
V, Å^3	5684.9(8)
Z	8
ρ(calcd.), g/cm^3	2.125
μ, mm^{-1}	11.655
F(000)	3416
Crystal size, mm	0.32 × 0.10 × 0.06
Data collection range of θ, deg	1.73–27.70
Ranges of reflection indices	$-10 \le h \le 10$, $-21 \le k \le 33$, $-36 \le l \le 33$
Number of measured reflections	32209
Number of unique reflections (R_{int})	6581 (0.0335)
Number of reflections with $I > 2\sigma(I)$	5311
Number of refinement parameters	270
GOOF	1.070
R_1, wR_2 on $F^2 > 2\sigma(F^2)$	0.0325, 0.0572
R_1, wR_2 for all reflections	0.0459, 0.0603
Residual electron density (min/max), e/Å^3	−2.350/1.776

squares (on F^2) in the full-matrix anisotropic approximation for non-hydrogen atoms. The positions of hydrogen atoms were calculated geometrically and included in the refinement in the riding model. The structure solution and refinement were carried out using the SHELXTL program package [27]. The key crystallographic data and structure refinement details for **IIa** are summarized in Table 1 and selected bond lengths and angles are in Table 2.

The atomic coordinates, bond lengths, bond angles, and the thermal parameters for complex **IIa** were deposited with the Cambridge Crystallographic Data Centre (CCDC no. 1978947; deposit@ccdc.cam.ac.uk or http://www.ccdc.cam.ac.uk).

RESULTS AND DISCUSSION

The ^{13}C CP-MAS NMR spectrum of the tetranuclear lead(II) complex $[Pb_4\{S_2CN(C_3H_7)_2\}_8]$ (**I**) exhibits resonance signals from the >NC(S)S–, >N–CH_2–, –CH_2–, and –CH_3 groups of the PrDtc ligands (Fig. 1a). The most informative region corresponding to dithiocarbamate groups shows two ^{13}C signals whose relative integral intensity ratio, close to 1 : 3, points to the presence of four nonequivalent ligands in **I**. Owing to higher sensitivity of ^{15}N CP-MAS NMR spectroscopy to small structural differences of the >NC(S)S– groups [24], it was possible to resolve resonance signals for each of the four structurally nonequivalent PrDtc ligands of complex **I** (Fig. 2). Each of the four ^{15}N signals (1 : 1 : 1 : 1) had two equidistant satellites due to the presence of ^{207}Pb nuclide (I = ½; magnetogyric ratio, γ = 5.58046 × 10^7 rad/(T s)) in natural lead. Since the natural abundance of ^{207}Pb is 22.1 at %, each of ^{15}N signals is a triplet (with calculated integral intensity ratio of 1 : 7 : 1), because of spin–spin couplings between ^{15}N and ^{207}Pb nuclei with $^3J(^{15}N–^{207}Pb)$ = 15–24 Hz. Thus, the set of ^{13}C and ^{15}N CP-MAS NMR data obtained for compound **I** is fully consistent with structural data for tetranuclear lead(II) dipropyldithiocarbamate [10].

The ^{13}C CP-MAS NMR spectrum of $[Au\{S_2CN(C_3H_7)_2\}_2][PbCl_3]$ (**II**), similarly to that of **I**, exhibits resonance signals for the chemical groups

Table 2. Bond lengths (d, Å) and bond (ω, deg) and torsion (φ, deg) angles in the structure of **IIa***

Bond	d, Å	Bond	d, Å
	Cation		
Au(1)–S(1)	2.3403(13)	S(3)–C(8)	1.730(5)
Au(1)–S(2)	2.3474(12)	S(4)–C(8)	1.737(5)
Au(1)–S(3)	2.3297(12)	N(1)–C(1)	1.307(6)
Au(1)–S(4)	2.3492(13)	N(1)–C(2)	1.479(7)
Au(1)···S(1)[a]	3.4378(14)	N(1)–C(5)	1.480(6)
Au(1)···S(4)[b]	3.5686(14)	N(2)–C(8)	1.311(6)
S(1)–C(1)	1.738(5)	N(2)–C(9)	1.482(6)
S(2)–C(1)	1.725(5)	N(2)–C(12)	1.484(7)
	Anion		
Pb(1)–Cl(1)	2.7496(13)	Pb(1)–Cl(1)[c]	3.0549(14)
Pb(1)–Cl(2)	3.1920(13)	Pb(1)–Cl(2)[c]	2.6830(12)
Pb(1)–Cl(3)	2.7640(12)	Pb(1)–Cl(3)[c]	3.1401(13)
	Toluene solvate molecule		
C(15)–C(16)	1.409(18)	C(16)–C(17)	1.331(19)
C(15)–C(17)	1.329(15)	C(15)–C(18)	1.495(10)
Angle	ω, deg	Angle	ω, deg
	Cation		
S(1)Au(1)S(2)	75.09(4)	Au(1)S(1)C(1)	86.81(17)
S(1)Au(1)S(3)	103.71(4)	Au(1)S(2)C(1)	86.89(17)
S(1)Au(1)S(4)	178.23(5)	Au(1)S(3)C(8)	87.39(17)
S(2)Au(1)S(3)	177.47(5)	Au(1)S(4)C(8)	86.61(17)
S(2)Au(1)S(4)	106.04(4)	S(1)C(1)S(2)	111.2(3)
S(3)Au(1)S(4)	75.11(4)	S(3)C(8)S(4)	110.7(3)
	Anion		
Cl(1)Pb(1)Cl(2)	81.34(4)	Cl(2)Pb(1)Cl(3)[c]	112.35(3)
Cl(1)Pb(1)Cl(3)	87.16(4)	Cl(3)Pb(1)Cl(1)[c]	96.49(4)
Cl(1)Pb(1)Cl(1)[c]	171.65(4)	Cl(3)Pb(1)Cl(2)[c]	91.44(4)
Cl(1)Pb(1)Cl(2)[c]	87.40(4)	Cl(3)Pb(1)Cl(3)[c]	168.57(4)
Cl(1)Pb(1)Cl(3)[c]	99.56(4)	Cl(1)[c]Pb(1)Cl(2)[c]	85.01(4)
Cl(2)Pb(1)Cl(3)	77.65(4)	Cl(1)[c]Pb(1)Cl(3)[c]	75.68(3)
Cl(2)Pb(1)Cl(1)[c]	106.75(3)	Cl(2)[c]Pb(1)Cl(3)[c]	79.72(4)
Cl(2)Pb(1)Cl(2)[c]	164.62(4)		
	Toluene solvate molecule		
C(15)C(16)C(17)	116.4(12)	C(16)C(15)C(17)	124.1(15)
C(15)C(17)C(16)	119.5(13)	C(16)C(15)C(18)	118.0(16)
Angle	ω, deg	Angle	ω, deg
Au(1)S(1)S(2)C(1)	177.3(3)	S(2)C(1)N(1)C(2)	178.8(4)
Au(1)S(3)S(4)C(8)	−174.6(3)	S(2)C(1)N(1)C(5)	−0.6(7)
S(1)Au(1)C(1)S(2)	177.5(3)	S(3)C(8)N(2)C(9)	−0.2(6)
S(3)Au(1)C(8)S(4)	−175.1(3)	S(3)C(8)N(2)C(12)	178.4(4)
S(1)C(1)N(1)C(2)	−1.1(7)	S(4)C(8)N(2)C(9)	−178.7(4)
S(1)C(1)N(1)C(5)	179.5(4)	S(4)C(8)N(2)C(12)	−0.1(7)

* Symmetry codes: [a] $1-x, y, 1/2-z$; [b] $-x, y, 1/2-z$; [c] $x-1/2, 1/2-y, -z$.

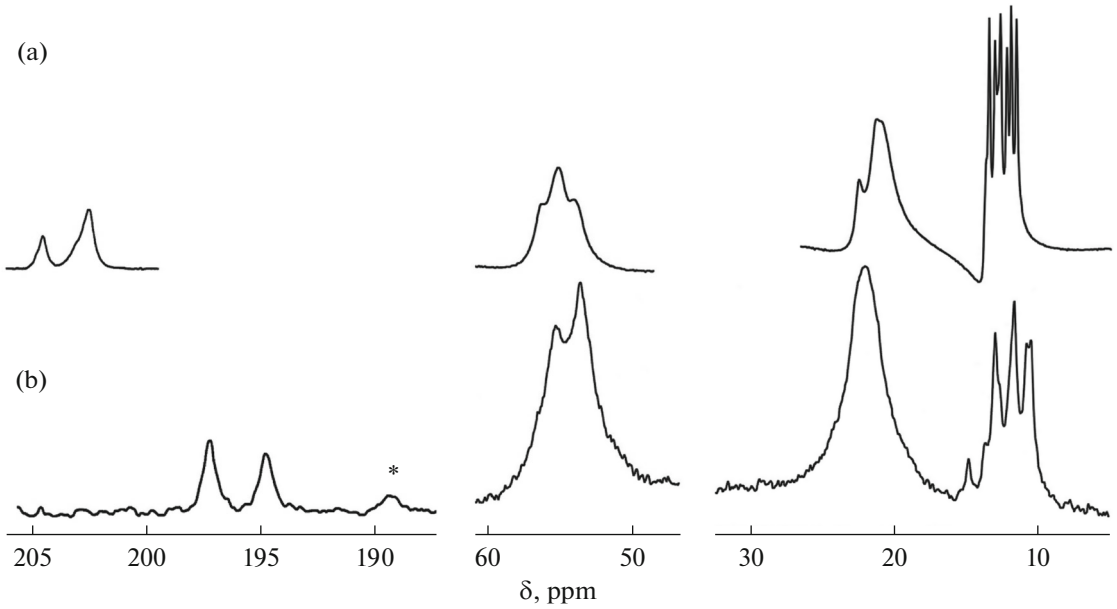

Fig. 1. ^{13}C CP-MAS NMR spectra of polycrystalline complexes (a) **I** and (b) **II**. Number of acquisitions/spinning frequency of samples (Hz): (a) 6100/5000 and (b) 10000/10100.

present in the PrDtc ligands (Fig. 1b). However, the crucial decrease in the ^{13}C chemical shift of >NC(S)S– groups in **II** (197.4 and 195.0 ppm) in comparison with that for **I** (204.6 and 202.5 ppm) indicates that the synthesis of **II** is accompanied by complete migration of PrDtc ligands into the gold(III) coordination sphere, as we noted for the previously prepared $[Au\{S_2CN(C_3H_7)_2\}_2][Cd_2Cl_6]$ (198.6 and 194.6 ppm) [28] and $[Au\{S_2CN(C_3H_7)_2\}_2][AgCl_2]$ (195.3 and 191.9 ppm) [29]. In addition, two equally intense (1 : 1) ^{13}C signals of dithiocarbamate groups in the spectrum of compound **II** attest to the presence of one non-centrosymmetric or two nonequivalent centrosymmetric $[Au\{S_2CN(C_3H_7)_2\}_2]^+$ cations in its structure. (Note that a weak ^{13}C signal (189.8 ppm; denoted in Fig. 1b by an asterisk) corresponding to an unidentified impurity is also present in the region of dithiocarbamate groups bound to gold.)

The most intense absorption band (1551 cm^{-1}) in the FT-IR spectrum of **II** corresponding to the ν(C–N) stretching modes of the >NC(S)S– groups of PrDtc occupies an intermediate position between the regions of single bond ν(C–N) (1360–1250 cm^{-1}) and double bond ν(C=N) (1690–1640 cm^{-1}) modes, which is indicative of a partially double nature of the C⋯N bond in the dithiocarbamate groups. It is noteworthy that the pronounced shift of this band to higher frequency with respect to that of the initial sodium salt $Na\{S_2CN(C_3H_7)_2\} \cdot H_2O$ (1468 cm^{-1} ν(C–N) [19]) is fully in line with the available data for complexes containing dithiocarbamate ligands coordinated to gold(III) in the *S*,*S*′-bidentate fashion [19, 30]. Absorption bands caused by asymmetric (ν_{as}) and symmetric (ν_s) stretching vibrations of the –C(S)S– groups were noted at 1161 and 968 cm^{-1}, respectively [31]. In turn, the most intense bands in the 2967–2871 cm^{-1} range were assigned to the CH_3– and $-CH_2-$ stretching modes of alkyl substituents [32]: 2967 $\nu_{as}(CH_3)$, 2871 $\nu_s(CH_3)$, and 2930 cm^{-1} $\nu_{as}(CH_2)$.

The structure of the solvated form of the double gold(III)–lead(II) ionic polymer complex was directly established by X-ray diffraction. The unit cell of **IIa** includes eight formula units $[Au\{S_2CN-$

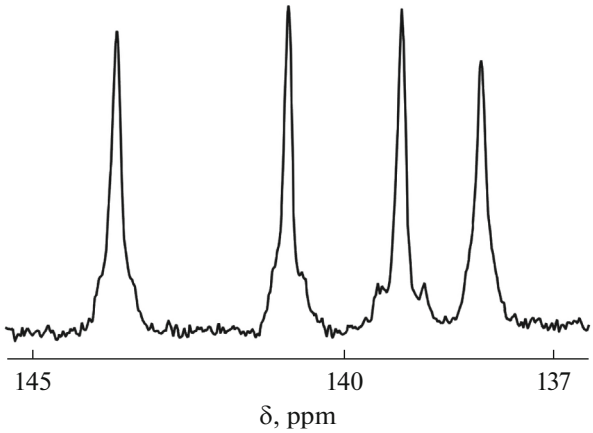

Fig. 2. ^{15}N CP-MAS NMR spectrum of polycrystalline sample **I**: number of acquisitions/spinning frequency of the sample (Hz): 12100/3750.

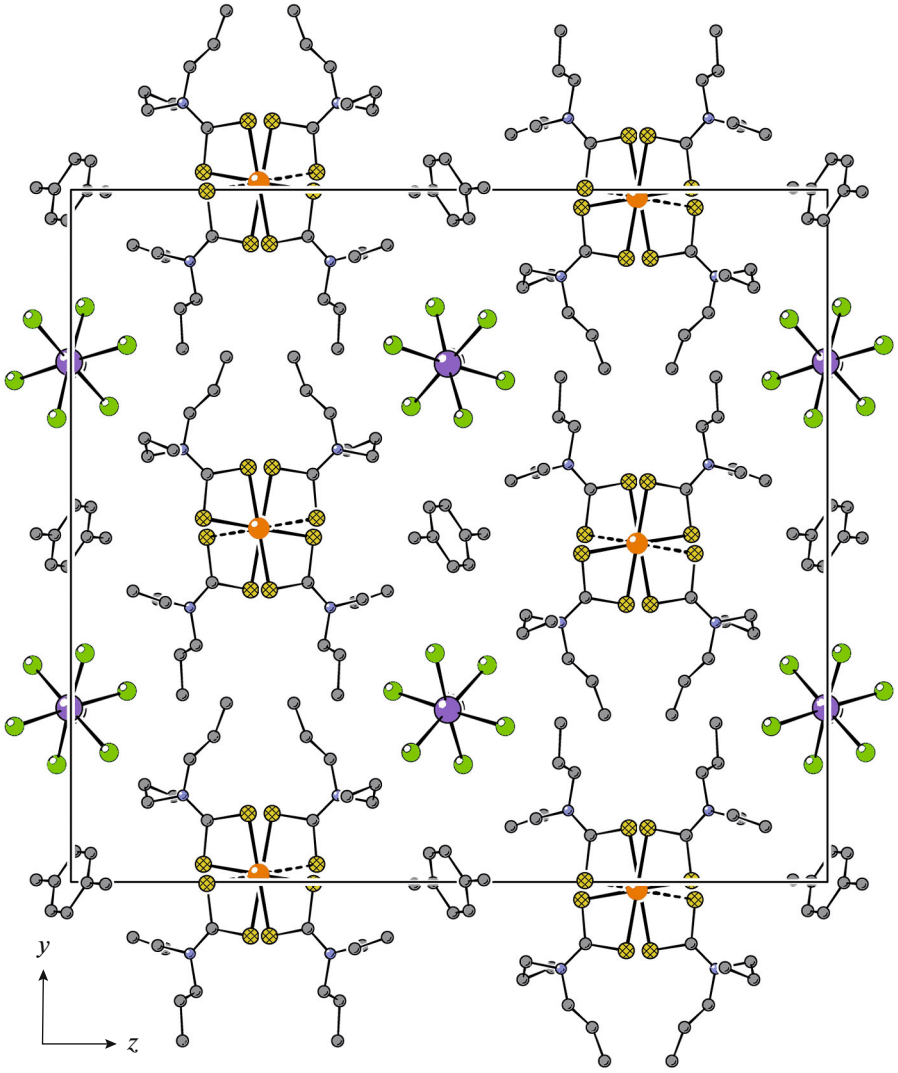

Fig. 3. Projection of the structure of **IIa** on the *yz* plane. The pseudo-polymer $([Au\{S_2CN(C_3H_7)_2\}_2]^+)_n$ and polymer $\{[Pb(\mu_2\text{-}Cl)_3]^-\}_n$ chains are extended along the *x* axis.

$(C_3H_7)_2\}_2][PbCl_3] \cdot 0.5CH_3\text{–}C_6H_5$ (Fig. 3). As was to be expected considering the ^{13}C CP-MAS NMR data, the cationic part of the complex is a non-centrosymmetric gold(III) complex ion $[Au\{S_2CN(C_3H_7)_2\}_2]^+$, which contains two nonequivalent PrDtc ligands. The coordination of one of the ligands is similar to *S*,*S*'-isobidentate one (Au–S, 2.3403 and 2.3474 Å), whereas the other ligand is prone to *S*,*S*'-anisobidentate coordination (Au–S, 2.3297 and 2.3492 Å). The bidentate coordination gives rise to two planar small-size four membered $[AuS_2C]$ metallacycles sharing the gold atom: the AuSSC and SAuCS torsion angles are close to 180° (Table 2); the Au···C distances are 2.836–2.838 Å and the S···S distances are 2.857–2.852 Å (the sums of the van der Waals radii of the corresponding pairs of atoms are 3.36 and 3.60 Å [33]). The proximate positions of the gold and carbon atoms in the $[AuS_2C]$ rings indicate the presence of *trans*-annular interaction between them. The diagonal SAuS angles do not differ much from 180° (Table 2), which attests to a coplanar arrangement of the atoms in the tetragonal $[AuS_4]$ chromophore, which is due to the low-spin intraorbital dsp^2-hybrid state of gold(III). The trapezoidal distortion of the discussed chromophore reflects the inequality of the long sides (3.673 and 3.752 Å) and the corresponding arrangement of obtuse (91.00°, 90.59°) and acute (89.07°, 89.33°) interior angles.

The $C_2NC(S)S$ groups in the PrDtc ligands are virtually planar: the SCNC torsion angles are close to 180° or 0° (Table 2). The dithiocarbamate groups are characterized by stronger N–C(S)S bonds (1.307 and 1.311 Å) compared to $N\text{–}CH_2$ (1.479–1.484 Å) (Table 2). Both these features point to a partially dou-

Table 3. Geometric parameters of hydrogen bonds in complex **IIa**

C–H···A contact	Distance, Å			Angle C–H···A, deg
	C–H	H···A	C···A	
C(6)–H(6*A*)···Cl(1)	0.99	2.71	3.632(6)	155
C(12)–H(12*B*)···Cl(1)	0.99	2.94	3.677(5)	132
C(9)–H(9*A*)···Cl(2)	0.99	2.86	3.628(5)	135
C(14)–H(14*B*)···Cl(2)	0.98	2.88	3.658(6)	137
C(5)–H(5*A*)···Cl(3)	0.99	2.75	3.652(5)	152
C(9)–H(9*A*)···Cl(3)	0.99	2.82	3.622(5)	139
C(13)–H(13*B*)···Cl(3)	0.99	2.93	3.836(5)	153

ble bond nature of the formally single N–C(S)S bond, which is attributable to partial admixing of the sp^2- to sp^3-hybrid state of the nitrogen and carbon atoms.

The structural self-organization of the cationic subsystem of complex **IIa** is determined by the secondary[2] non-valent Au···S interactions (Fig. 4b). For each $[Au\{S_2CN(C_3H_7)_2\}_2]^+$ complex cation, asymmetric interactions with two neighbors involve the triad of atoms of the [S(1)–Au(1)–S(4)] linear structural moiety (Fig. 4a). This gives rise to two pairs of nonequivalent secondary bonds: Au(1)···S(1)^a, Au(1)^a···S(1) (3.4378 Å) and Au(1)···S(4)^b, Au(1)^b···S(4) (3.5686 Å) (the sum of the van der Waals radii of the gold and sulfur atoms is 3.46 Å [33]). These cation–cation interactions give rise to supramolecular pseudo-1D-polymer chains $([Au\{S_2CN(C_3H_7)_2\}_2]^+)_n$ (Au(1)^{a}Au(1)Au(1)^b, 177.172(9)°; Au(1)–Au(1)^a, 3.9140(5) Å; and Au(1)–Au(1)^b, 3.8553(5) Å), extended along the crystallographic *x* axis (Fig. 3).

In these pseudo-polymer chains, the difference between the spatial arrangements of the alternating cations can be quantitatively characterized by the angle between the bisecting planes (that separate the bicyclic $[CS_2AuS_2C]$ moieties in the neighboring cations), which is close to a right angle (88.7(7)°). The angle between the planes of the $[AuS_4]$ chromophores of the neighboring cations is 19.19(3)°. The secondary Au···S bonds complete the gold polyhedron to a distorted, highly elongated $[AuS_{4+2}]$ octahedron (S(1)^a···Au(1)···S(4)^b, 176.98(3)°), in which the axial sulfur atoms are displaced from ideal positions, since the S(1)^a···Au(1)–C(8) (80.3(1)°) and S(4)^b···Au(1)–S(1) angles (81.70(4)°) markedly deviate from 90°.

[2] The concept of secondary bonds proposed in [34] interprets the interactions between two atoms located at distances compared with the sums of their van der Waals radii.

The anionic part of the complex is composed of 1D polymeric tri(μ_2-chloro)plumbate(II) ion, $\{[Pb(\mu_2\text{-}Cl)_3]^-\}_n$, in which the lead atoms are combined with each of two nearest neighbors by three nonequivalent μ_2-bridging chlorine atoms (Fig. 5). The latter are characterized by asymmetric coordination to neighboring metal atoms, each forming two Pb–Cl bonds with considerably different lengths (Table 2). The formation of these bonds gives rise to a zigzag-like anionic polymer chain (Pb(1)^{a}Pb(1)Pb(1)^b, 175.746(6)°; Pb(1)–Pb(1)^a 3.8862(4) Å) extended along the crystallographic *x* axis. Each lead atom in the chain has a six-chlorine $[PbCl_6]$ environment, thus forming six nonequivalent Pb–Cl bonds, three of which are shorter (2.6830–2.7640 Å) than the other three (3.0549–3.1920 Å). The former are comparable with the sum of empirical covalent radii of the lead and sulfur atoms (2.46 Å [35]), while considerable weakening of the latter points to a pronounced contribution of the ionic component [36]. The metal polyhedron can be approximated by a highly distorted octahedron [36, 37] or a trigonal antiprism whose bases defined by the Cl(1)–Cl(3) and Cl(1)^a–Cl(3)^a chlorine atoms (Fig. 5) are not quite parallel: the angle between the corresponding planes is 38.75(4)°.

The cationic pseudo-polymer and anionic polymer chains interact via numerous C–H···Cl contacts (Table 3). As a result, pairs of cationic and anionic chains spatially determine channels occupied by solvating toluene molecules in the crystal structure of **IIa**. The molecules are randomly distributed between two positions with equal occupancies and have methyl substituents pointing to opposite directions (Fig. 3).

Thus, the Au(III)–Pb(II) double complex was obtained an individual form of gold(III) binding from solution by the tetranuclear lead(II) dipropyldithiocabmate $[Pb_4\{S_2CN(C_3H_7)_2\}_8]$; whereas, upon crystallization from an acetone-toluene solution, the

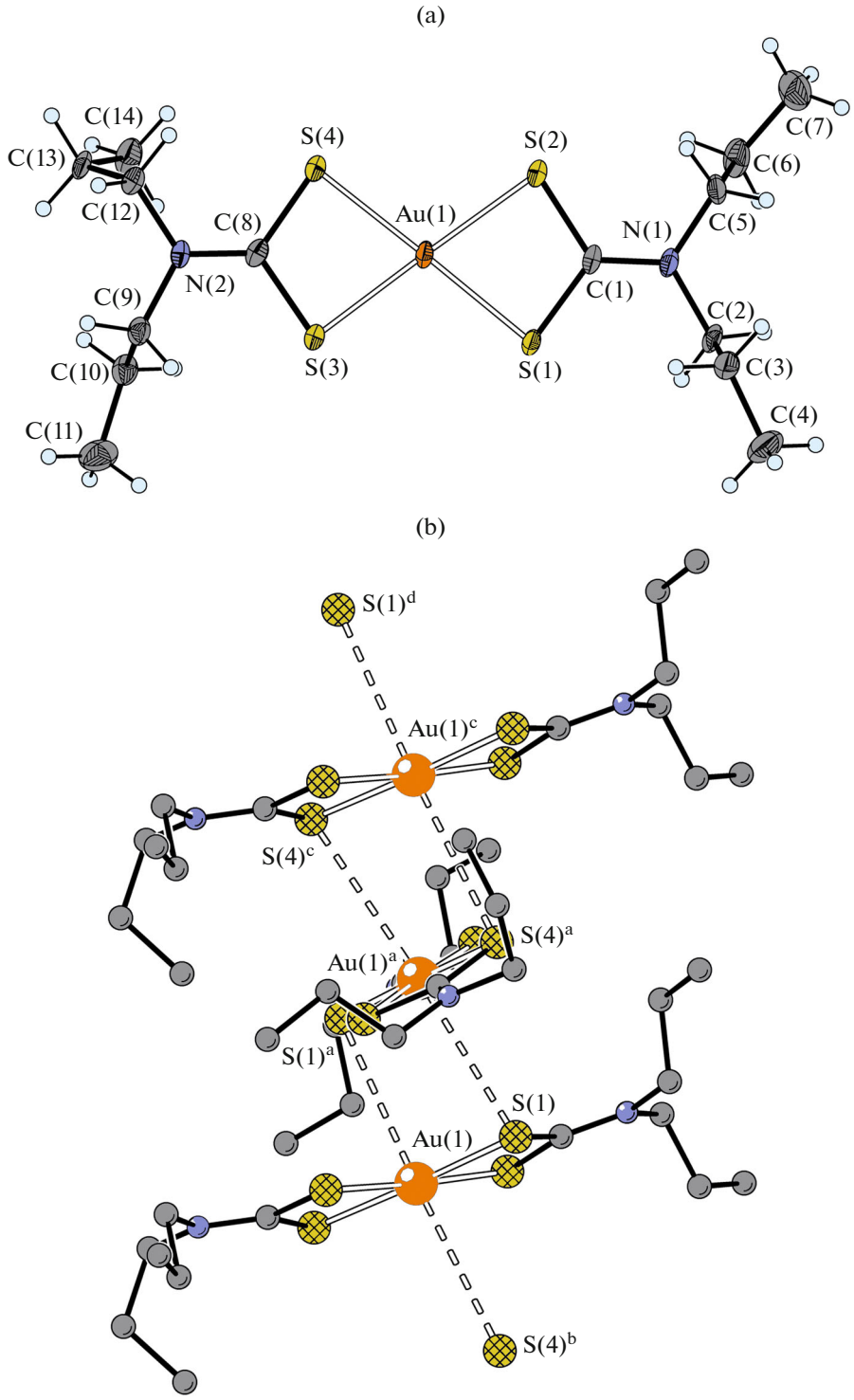

Fig. 4. (a) Structure of the non-centrosymmetric complex cation $[Au\{S_2CN(C_3H_7)_2\}_2]^+$, ellipsoids are drawn at 50% probability level and (b) a three-membered fragment of the supramolecular pseudo-polymer chain $([Au\{S_2CN(C_3H_7)_2\}_2]^+)_n$. The double dashed lines show secondary Au···S bonds between cations; symmetry codes: [a] $1-x, y, 1/2-z$; [b] $-x, y, 1/2-z$; [c] $1+x, y, z$; [d] $2-x, y, 1/2-z$.

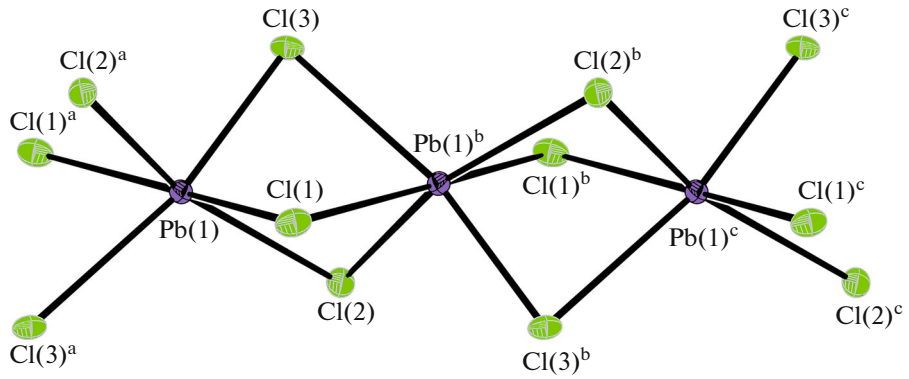

Fig. 5. A three-membered fragment of the anionic polymer chain $([PbCl_3]^-)_n$. The ellipsoids are drawn at 50% probability level; symmetry codes: [a] $x - 1/2, 1/2 - y, -z$; [b] $1/2 + x, 1/2 - y, -z$; [c] $1/2 + x, y, z$.

resulting complex gives a solvated ionic polymer compound of $([Au\{S_2CN(C_3H_7)_2\}_2][PbCl_3] \cdot 0.5CH_3C_6H_5)_n$. In the cationic subsystem, pairs of nonequivalent secondary Au···S bonds combine non-centrosymmetric gold(III) complex ions into supramolecular pseudo-polymer chain $([Au\{S_2CN(C_3H_7)_2\}_2]^+)_n$. The trichloroplumbate(II) ion also exists as a 1D polymeric form of $\{[Pb(\mu_2\text{-}Cl)_3]^-\}_n$. The system of C–H···Cl hydrogen bonds between the cationic and anionic chains promotes the formation of channels in the crystal lattice occupied by disordered solvating toluene molecules.

ACKNOWLEDGMENTS

The authors are grateful to Prof. O.N. Antzutkin (Luleå University of Technology, Sweden) for kindly providing the possibility to record solid-state ^{13}C and ^{15}N NMR spectra.

CONFLICT OF INTEREST

The authors declare that they have no conflicts of interest.

REFERENCES

1. Dhar, A., Dey, A., Maiti, P., et al., *Ionics*, 2018, vol. 24, no. 4, p. 1227.
2. Hassan, H.E., Badran, H.M., Aydarous, A., and Sharshar, T. *Nucl. Instrum. Methods Phys. Res. B*, 2015, vol. 360, p. 81.
3. Raza, W., Wu, H., Xu, Y., and Qirong, Sh., *J. Chem. Soc. Pak.*, 2011, vol. 33, no. 2, p. 193.
4. Nyamen, L.D., Rajasekhar Pullabhotla, V.S.R., Nejo, A.A., et al, *Dalton Trans.*, 2012, vol. 41, no. 27, p. 8297.
5. Sathiyaraj, E. and Thirumaran, S., *Spectrochim. Acta, Part A*, 2012, vol. 97, p. 575.
6. Lewis, E.A., McNaughter, P.D., Yin, Zh., et al., *Chem. Mater.*, 2015, vol. 27, no. 6, p. 2127.
7. Chintso, T. and Ajibade, P.A., *Mater. Lett.*, 2015, vol. 141, p. 1.
8. Iwasaki, H., *Acta Crystallogr., Sect. B: Struct. Crystallogr. Cryst. Chem.,* 1980, vol. 36, no. 9, p. 2138.
9. Iwasaki, H. and Hagihara, H., *Acta Crystallogr., Sect. B*: *Struct. Crystallogr. Cryst. Chem.*, 1972, vol. 28, no. 2, p. 507.
10. Bharadwaj, P.K., Arbuckle, B.W., and Musker, W.K., *Inorg. Chim. Acta*, 1988, vol. 142, no. 2, p. 243.
11. Ito, M. and Iwasaki, H., *Acta Crystallogr., Sect. B*: *Struct. Crystallogr. Cryst. Chem.*, 1980, vol. 36, no. 2, p. 443.
12. Angeloski, A., Gentle, A.R., Scott, J.A., et al., *Inorg. Chem.*, 2018, vol. 57, no. 4, p. 2132.
13. Afzaal, M., Ellwood, K., Pickett, N.L., et al., *J. Mater. Chem.*, 2004, vol. 14, no. 8, p. 1310.
14. Akhtar, J., Malik, M.A., O'Brien, P., and Helliwell, M., *J. Mater. Chem.*, 2010, vol. 20, no. 29, p. 6116.
15. Trindade, T., O'Brien, P., Zhang, X.-M., and Motevalli, M., *J. Mater. Chem.*, 1997, vol. 7, no. 6, p. 1011.
16. Oluwalana, A.E. and Ajibade, P.A., *J. Sulfur Chem.*, 2019, vol. 41, no. 2, p. 182.
17. Caruso, F., Chan, M.-L., and Rossi, M., *Inorg. Chem.*, 1997, vol. 36, no. 17, p. 3609.
18. Trindade, T., Monteiro, O.C., O'Brien, P., and Motevalli, M., *Polyhedron*, 1999, vol. 18, nos. 8–9, p. 1171.
19. Ivanov, A.V., Gerasimenko, A.V., Egorova, I.V., et al., *Russ. J. Coord. Chem.*, 2018, vol. 44, no. 8, p. 518. https://doi.org/10.1134/S1070328418080043
20. Zaeva, A.S., Ivanov, A.V., Gerasimenko, A.V., and Sergienko, V.I., *Russ. J. Inorg. Chem.,* 2015, vol. 60, no. 2, p. 203. https://doi.org/10.7868/S0044457X15020233
21. Ivanov, A.V., Bredyuk, O.A., and Loseva, O.V., *Russ. J. Gen. Chem.,* 2018, vol. 88, no. 7, p. 1470. https://doi.org/10.1134/S1070363218070198
22. Bredyuk, O.A., Loseva, O.V., Ivanov, A.V., et al., *Russ. J. Coord. Chem.,* 2017, vol. 43, no. 10, p. 638. https://doi.org/10.1134/S1070328417100013
23. Byr'ko, V.M., *Ditiokarbamaty* (Dithiocarbamates), Moscow: Nauka, 1984.
24. Ivanov, A.V. and Antzutkin, O.N., *Top. Curr. Chem.*, 2005, vol. 246, p. 271.

25. Pines, A., Gibby, M.G., and Waugh, J.S., *J. Chem. Phys.*, 1972, vol. 56, no. 4, p. 1776.
26. Ratcliffe, C.I., Ripmeester, J.A., and Tse, J.S., *Chem. Phys. Lett.*, 1983, vol. 99, no. 2, p. 177.
27. *APEX2 (version 1.08), SAINT (version 7.03), SADABS (version 2.11), SHELXTL (version 6.12)*, Madison: Bruker AXS Inc., 2004.
28. Rodina, T.A., Ivanov, A.V., Gerasimenko, A.V., et al., *Polyhedron*, 2012, vol. 40, no. 1, p. 53.
29. Korneeva, E.V., Smolentsev, A.I., Antzutkin, O.N., and Ivanov, A.V., *Russ. Chem. Bull. Int. Ed.*, 2019, vol. 68, no. 1, p. 40. https://doi.org/10.1007/s11172-019-2413-7
30. Loseva, O.V., Rodina, T.A., Ivanov, A.V., et al., *Russ. J. Coord. Chem.,* 2018, vol. 44, no. 10, p. 604. https://doi.org/10.1134/S107032841810007X
31. Yin, H.D., Li, F., and Wang, D., *J. Coord. Chem.*, 2007, vol. 60, no. 11, p. 1133.
32. Gremlikh, G.U. *Yazyk spektrov. Vvedenie v interpretatsiyu spektrov organicheskikh soedinenii* (The Language of Spectra. Introduction to Interpretation of the Spectra of Organic Compounds), Moscow: LLC Bruker Optik, 2002.
33. Bondi, A., *J. Phys. Chem.*, 1964, vol. 68, no. 3, p. 441.
34. Alcock, N.W., Adv. *Inorg. Chem. Radiochem.*, 1972, vol. 15, no. 1, p. 1.
35. Winter, M., Web Elements Periodic Table of the Elements. http://www.webelements.com.
36. Corradi, A.B., Bruni, S., Cariati, F., et al., *Inorg. Chim. Acta*, 1997, vol. 254, no. 1, p. 137.
37. Ramalingam, K., Rizzoli, C., Rajaraman, T., and Prabu, M., *Main Group Met. Chem.,* 2016, vol. 39, nos. 5–6, p. 175.

Translated by Z. Svitanko